Interaction of an Antimicrobial Peptide with Membranes: Experiments and Simulations with NKCS

Yana Gofman,[†] Sebastian Linser,[†] Agnieszka Rzeszutek,[†] Dalit Shental-Bechor,[‡] Sergio S. Funari,[§] Nir Ben-Tal,*[,‡] and Regine Willumeit*[,†]

GKSS Research Center, 21502 Geesthacht, Germany, Department of Biochemistry, The George S. Wise Faculty of Life Sciences, Tel-Aviv University, Ramat-Aviv, 69978 Tel-Aviv, Israel, and Hasylab, DESY, 22603 Hamburg, Germany

Received: September 23, 2009; Revised Manuscript Received: January 6, 2010

We used Monte Carlo simulations and biophysical measurements to study the interaction of NKCS, a derivative of the antimicrobial peptide NK-2, with a 1-palmitoyl-2-oleoyl-*sn*-glycero-3-phosphoethanolamine (POPE) membrane. The simulations showed that NKCS adsorbed on the membrane surface and the dominant conformation featured two amphipathic helices connected by a hinge region. We designed two mutants in the hinge to investigate the interplay between helicity and membrane affinity. Simulations with a Leu-to-Pro substitution showed that the helicity and membrane affinity of the mutant (NKCS-[LP]) decreased. Two Ala residues were added to NKCS to produce a sequence that is compatible with a continuous amphipathic helix structure (NKCS-[AA]), and the simulations showed that the mutant adsorbed on the membrane surface with a particularly high affinity. The circular dichroism spectra of the three peptides also showed that NKCS-[LP] is the least helical and NKCS-[AA] is the most. However, the activity of the peptides, determined in terms of their antimicrobial potency and influence on the temperature of the transition of the lipid to hexagonal phase, displayed a complex behavior: NKCS-[LP] was the least potent and had the smallest influence on the transition temperature, and NKCS was the most potent and had the largest effect on the temperature.

Introduction

After half a century of almost complete control over microbial infections, the past decade has brought a worldwide resurgence of infectious diseases due to the evolution of antibiotic-resistant strains at an alarming rate.[1,2] As a potential class of novel antimicrobial agents, animal-derived antimicrobial peptides (AMP) have recently emerged.[3−5] These peptides are fast and lethal toward a broad spectrum of pathogens but are quite harmless to eukaryotic cells. Some AMPs also possess anticancer and antiviral activity, as well as the capacity to manipulate the innate immune response.[3] The first generation of antimicrobial peptides is already at the edge of application.[4,6] However, the dose effective in vitro is very close to the toxic dose in animal models, indicating that a concerted effort to understand the interaction of antibacterial peptides with their target membrane is of utmost importance.

The precise mechanism of action of antimicrobial peptides and the molecular basis for their selective cytotoxicity are not fully understood. Data suggest that, regardless of their origin and the diversity in their primary and secondary structure, the antimicrobial activity of the peptides is a result of direct interactions with the phospholipids of the pathogens' membrane rather than association with a specific receptor. It is generally believed that most antimicrobial peptides lyse their target cell by the destabilization of the cytoplasmic membrane.[3,7−10] The selectivity of the cytolytic mechanism is assumed to stem from inherent differences in the lipid composition of the target cells.[10]

The NK-2 peptide, corresponding to residues 39−65 of the NK-lysin protein, has been investigated extensively due to its high antimicrobial[11−13] and anticancer qualities[14] as well as low hemolytic activity.[11] The peptide was found to reduce the transition temperature of the lipid bilayer in a concentration dependent manner by up to 10 °C.[15] The replacement of cysteine residue within the NK-2 sequence with a serine (C7S), resulted in a peptide with an improved antibacterial activity referred to as NKCS in the current study.[16] Both peptides are randomly coiled in water and adopt a helical structure upon interaction with the lipid bilayer.[11,16]

Several approaches are used to investigate the interaction between antibacterial peptides and lipid membranes. These include biophysical studies using techniques such as differential scanning calorimetry (DSC),[17] Fourier transform infrared (FTIR) spectroscopy,[18] circular dichroism (CD) spectroscopy,[19] scattering techniques (X-ray and neutron scattering),[17,20] NMR,[21] and surface plasmon resonance (SPR),[22] as well as computational studies including molecular dynamics simulations,[23,24] continuum solvent models,[25,26] and Monte Carlo (MC) simulations.[27−34] In this work we characterized the interactions between the cationic peptide NKCS and 1-palmitoyl-2-oleoyl-*sn*-glycero-3-phosphoethanolamine (POPE) membranes. We employed small-angle X-ray scattering (SAXS) and SPR along with measurements of the antibacterial and hemolytic activity in cells. We used CD spectroscopy to estimate the peptide's helicity. In addition, we performed MC simulations of NKCS and its derivatives in a POPE membrane.[35−38]

Phosphoethanolamine (PE) is a prominent example for the capability of a lipid to create nonbilayer forms such as hexagonal phases. Under suitable conditions even cubic structures are formed.[39,40] The local formation of nonbilayer structures is a prerequisite for the fusion and division of cell membranes when,

* Corresponding authors. E-mail: N.B.-T., NirB@tauex.tau.ac.il; R.W., Regine.Willumeit@gkss.de.
[†] GKSS Research Center.
[‡] Tel-Aviv University.
[§] Hasylab.

10.1021/jp909154y
Published on Web 03/04/2010

TABLE 1: Amino Acid Sequences of the Peptides

NKCS	KILRGVSKKIMRT	FLRRISKDILTGKK
NKCS-[LP]	KILRGVSKKIMRT	F**P**RRISKDILTGKK
NKCS-[AA]	KILRGVSKKIMRT**AA**FLRRISKDILTGKK	

[a] The changes are marked in bold fonts.

for very short periods of time, these structures are built in a living system.[41] The fraction of PE in the cytoplasmic membrane varies between, e.g., 69% of the total phospholipid in *Escherichia coli*,[42] 10% in *Bacillus subtilis*,[43] and 0% in *Staphylococcus aureus*.[44] Even though PE is not always the most abundant lipid in bacterial membranes, it interacts strongly with cationic peptides, leading to changes in the phase transition temperature. Specifically, magainin[45] and its analog MSI-78[46] show a significant increase in the lipid hexagonal phase transition temperature, whereas gramicidin,[47] alamethicin,[48] and the wasp venom peptide mastoparan[49] reduce the temperature.

The central hypothesis of this paper is that simple structural features, such as α-helicity and amphipathicity can be used to interpret changes in the membrane affinity of NKCS. We design two mutants, NKCS-[AA] and NKCS-[LP], to examine it, and to correlate the membrane affinity and activity of the peptides. We show that NKCS, NKCS-[AA], and NKCS-[LP] are, in essence, random coils in the aqueous solution. Upon membrane association, NKCS and NKCS-[AA] assume helical conformations, while the helical content of NKCS-[LP] stays low. This is demonstrated both in the CD spectroscopy studies and in the simulations. However, the assumption that the biological activity of a peptide increases with its membrane affinity might not always be true. For example, NKCS-[AA] and NKCS-[LP] manifest similar activities despite significant changes in the values of their calculated membrane-association free energies.

Theoretical Calculations

Monte Carlo simulations of the interaction of a peptide molecule with POPE membranes were performed as described previously.[35−38] The peptide was described using a reduced representation with each amino acid represented as two interaction sites, one corresponding to the α-carbon and the other to the side chain. The initial conformations of the peptides were modeled using the Nest program,[50] based on the structure of NK-lysin from the Protein Data Bank (entry 1NKL, model 1). The lipid membrane was approximated as a hydrophobic profile, corresponding to the hydrocarbon region of the membrane. The model membrane included also surface charges, corresponding to the polar headgroups, which interacted electrostatically with the titratable residues of the peptide, depending on their protonation state, using the Gouy−Chapman potential. A more detailed computational protocol is available in the Supporting Information.

Materials and Methods

Peptides. The peptide NKCS and its derivatives were synthesized by Biosyntan (Berlin, Germany). All three peptides carry a net charge of +10 (calculated by counting the N-terminus, lysine, histidine, and arginine as positive charges and counting aspartate as a negative charge; the C-termini are amidated). The sequences are shown in Table 1. The choice of peptides is explicated in Discussion. The purity of 95% was guaranteed by analytical RP-HPLC (Lichrospher 100 RP 18, 5 μm columns, Merck, Darmstadt, Germany) and MALDI-TOF (Bruker Daltonik GmbH, Bremen, Germany) performed by the company.

Melittin was purchased from Sigma-Aldrich (Deisenhofen, Germany). It was used to compare its known hemolytic activity with that of the investigated peptides.[51]

The peptides were stored at −20 °C. Directly before use they were dissolved in double distilled water to a final concentration of 1 mM. Between the experiments the peptide solutions were also stored at −20 °C.

Lipid. The phospholipid POPE was purchased from Sigma-Aldrich (Deisenhofen, Germany) and stored airtight in the freezer at −20 °C.

Circular Dichroism (CD). CD data were acquired with a JASCO CD spectrophotometer (JASCO, Gross-Umstadt, Germany) using quartz cuvettes with an optical path length of 0.1 cm. The CD was measured between 260 and 185 nm with a 0.5 nm step resolution and a 1 nm bandwidth. The counting rate was 50 nm/min with 4 s response time. Each spectrum was a sum of at least three scans to improve the signal/noise ratio. The detergent, sodium dodecyl sulfate (SDS) (Fluka, St. Louis, MO), which mimics some characteristics of biological membranes, was added to the cuvette with final concentrations of 1 and 10 mM in double distilled water before the peptides were added. As references, the spectra of double distilled water and SDS at the respective concentration were subtracted from the measurements with peptides. All spectra were collected for a concentration of 60 μM peptide in double distilled water. The molar ratio of peptide to SDS was 1:17 (for 1 mM SDS) and 1:167 (10 mM SDS).

Surface Plasmon Resonance (SPR). Surface plasmon resonance phenomenon allows performing the real-time measurements of the adhesion of molecules to the biomimetic surfaces. The SPR detector detects the changes in optical properties at the sensor surface coated with the ligand due to the adsorption and desorption of the solute.[52]

The SPR apparatus BIAcore X (GE Healthcare, Freiburg, Germany) was equipped with an internal injection system (500 μL Hamilton syringe). The running buffer was a 10 mM sodium phosphate buffer (pH 7.4), and the flow rate was 5 μL/min for all experiments. We used the BIAcore L1 chip, which was composed of a thin dextran matrix modified by lipophilic compounds on a gold surface where the lipid vesicles could be captured.[53] All solutions were freshly prepared, degassed, and filtered through 0.22 μm pores. The experiments were done at the room temperature (RT). After the system was cleaned according to the manufacturer's instructions, the BIAcore X apparatus was left running overnight using Milli-Q water as eluent to thoroughly wash all liquid-handling parts of the instrument. The L1 chip was then installed, and the surface was cleaned by an injection of the nonionic detergent *N*-octyl β-D-glucopyranoside (50 μL, 40 mM).

The phospholipid POPE was dissolved in a methanol/chloroform (Merck, Darmstadt, Germany) (1/2, v/v) solution. The solvent was slowly removed by a constant stream of nitrogen. The resulting lipid film was dried in a vacuum oven at 40 °C overnight. Just before the experiments, the lipid films were hydrated in buffer. To form multilamellar vesicles of POPE, sodium phosphate buffer (Merck, Darmstadt, Germany) was added at the room temperature to the lipid films and a small amount of glass beads was put into the vials. After vortexing for 1 min, the solution was incubated for 2 h at 28 °C, while every 30 min the sample was vortexed. Then the solution was cooled to RT and POPE vesicles (100 μL, 1 mM) were applied to the chip surface. To remove artifacts, NaOH (5 μL, 10 mM) was injected, which resulted in a stable baseline corresponding to the lipid bilayer linked to the chip surface. The thickness of

TABLE 2: Average Binding Free Energy and Fraction of All, "Inner" and "Outer" Conformations of NKCS, NKCS-[LP], and NKCS-[AA] Predicted by the MC Simulations[a]

peptide	conformations	calculated membrane-association energy (kT)	fraction (%)	measured membrane-association energy (kT)
NKCS	inner	-21.6 ± 1.8	85 ± 3	
	outer	-6.5 ± 0.7	15 ± 3	
	all	-20.5 ± 1.9	100	-18.5 ± 1.1 ($n = 6$)
NKCS-[LP]	inner	-17.3 ± 1.6	64 ± 2	
	outer	-10.9 ± 1.0	36 ± 2	
	all	-16.0 ± 1.0	100	-16.1 ± 0.3 ($n = 5$)
NKCS-[AA]	inner	-34.3 ± 0.4	99.8 ± 0.2	
	outer	38.9 ± 19.0	0.2 ± 0.2	
	all	-34.3 ± 0.4	100	-25.7 ± 0.3 ($n = 5$)

[a] For comparison, the average binding energies of the peptides to POPE measured using SPR are presented in the last column. The number of experiments, n, is indicated in parentheses. All values are shown as average $\pm$ standard deviation.

the bilayer was calculated by assuming that 1000 RU (response units) correspond to 1 nm layer thickness.[54] This bilayer was subsequently used as a model membrane surface to study the peptide−membrane interactions. For all peptides, 50 μL of a 1 μM solution was injected while the adsorption and desorption of the peptide was observed until it resulted in a stable signal. Finally, NaOH was injected to wash all unbound compounds away. All measurements were performed in triplicates.

Small Angle X-ray Scattering (SAXS). The POPE vesicles were prepared as described above with a final concentration of 25 mg/mL. After 30 min at room temperature, mixing with the appropriate peptide solution followed. The measurements were performed at the A2 beamline at HASYLAB, DESY. It ran with a wavelength $\lambda = 0.15$ nm and covered a scattering vector $s = 1/d = (2 \sin \theta)/\lambda$ (2θ = scattering angle, d = lattice spacing) from 1×10^{-2} to 0.5 nm^{-1}. The calibration for the SAXS pattern was done by measuring rat tail tendon (repeat distance 65 nm, standard at beamline A2) in addition to silver behenate ($[CH_3(CH_2)_2OCOO-Ag]$, repeat distance 5.838 nm, made available at beamline A2). The samples were measured in a temperature-controlled sample holder, where the temperature was varied with an increase of 2 °C/min and the data were collected for 10 s per measurement.

The data were normalized with respect to the primary beam and the background (buffer measurement). The positions of the diffraction peaks were determined using the OTOKO software.[55] The repeat distances were calculated from the peak positions based on the rat tail tendon and silver behenate calibration.

Antibacterial Assay. The *Escherichia coli* strain K12 (ATCC 23716), the *Staphylococcus carnosus* strain (ATCC 51365), and the *Bacillus subtilis* strain (ATCC 6051) (all bacteria were obtained from DSMZ, Braunschweig, Germany) were cultivated in the respective medium at 37 °C with shaking at 160 rpm to reach the log-phase. The peptides were 2-fold serial diluted and 10 μL of the log-phase bacteria suspension containing 100 colony forming units (CFU) was added to 90 μL of the peptide solution to measure the antibacterial activity by a microdilution susceptibility test. The density of the bacteria suspension was measured photometrically at 620 nm wavelength with a microplate reader (Tecan, Crailsheim, Germany). Values of the minimal inhibitory concentration (MIC) were defined as the concentration of the highest dilution of the peptides at which the bacteria growth was completely suppressed.

Hemolysis. To measure the hemolytic activity of the peptides, fresh (maximum storage time was 2 days) human blood (group 0 rhesus positive), was centrifuged for 3 min at 2000 rpm. The supernatant was discarded and the pellet washed with phosphate buffered saline (PBS) three times. The erythrocytes pellet was subsequently diluted with MES buffer (20 mM morpholinoethanesulfonic acid, 140 mM NaCL, pH 5.5 (Merck, Darmstadt, Germany)) until 20 μL of this suspension added to 980 μL of double distilled water gave the absorbance 1.4 at the wavelength of 412 nm, which equaled 5×10^8 cells/mL. The peptides were diluted in MES buffer to the desired concentrations before 20 μL of the erythrocyte suspension was added to 80 μL of peptide solution. As the control, 20 μL of erythrocyte suspension was mixed with 80 μL of double distilled water, expecting 100% lysis of the erythrocytes. The negative control was made by mixing 20 μL of erythrocyte suspension and 80 μL of MES buffer. After all samples were carefully mixed, the suspensions were incubated for 30 min at 37 °C. Directly after incubation the samples were stored on ice and MES buffer (900 μL) was added. All suspensions were centrifuged for 10 min at 2000 rpm to separate intact erythrocytes. Finally, the absorbance was measured with a spectrometer (Tecan, Crailsheim, Germany) at 412 nm wavelength.

Simulation Results

We conducted preliminary MC simulations of NKCS in the aqueous phase and within a POPE membrane and analyzed the structural and free energy determinants of the membrane association. The peptide adsorbed on the membrane surface with an association free energy of -20.5 kT (Table 2). A close look at the predicted conformations of the peptide showed a mixture of two main groups (Figure 1A). In the first (Figure 1A), which we called "the inner group of conformations", the peptide was partially dissolved in the membrane. The nonpolar residues were immersed in the hydrophobic region of the membrane, whereas the polar and charged residues were located in water, in close proximity to the membrane surface charge. Most of the conformations were helical with a distortion (hinge) in residues Thr-13 and Phe-14 (Figure 1B). In the second, outer, group of NKCS conformations, the peptide was randomly coiled and located, in essence, outside the membrane. This group of conformations resembled in its low helix content the conformations that were observed in the aqueous phase. The lysine and arginine residues pointed toward the slightly negatively charged membrane surface, whereas the nonpolar residues of the peptide faced the aqueous phase and did not interact with the membrane.

The free energy of membrane-association of the NKCS "inner" conformations was significantly lower (i.e., more favorable) than that of the "outer" ones (Table 2). Free energy decomposition suggested that the difference is mainly due to desolvation of the nonpolar residues (Supporting Information Table S1). These were embedded in the membrane in the inner conformations and interacted favorably with the hydrocarbon region whereas in the outer conformations they faced the solvent.

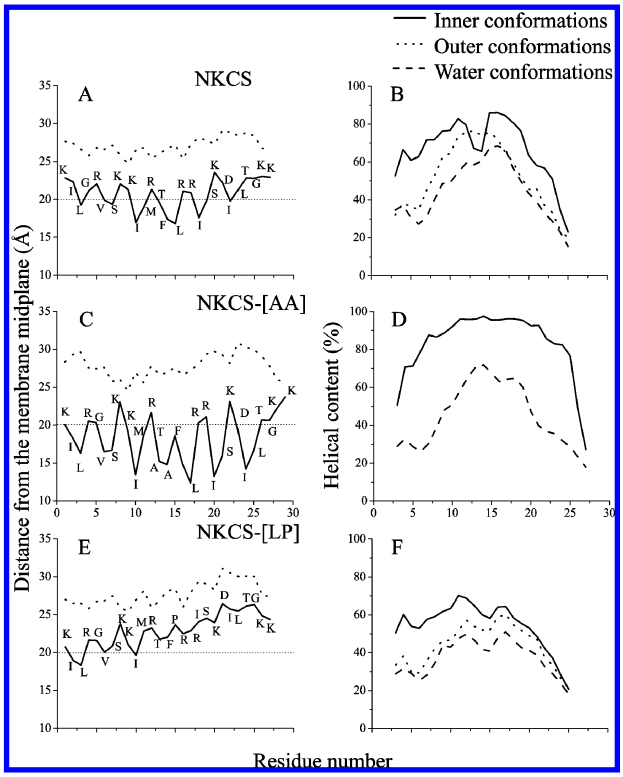

Figure 1. Location of the inner and outer conformations of (A) NKCS, (C) NKCS-[AA], and (E) NKCS-[LP] near the membrane. The average distance of the α-carbon atoms from the membrane midplane in the MC simulations is shown for each residue. The horizontal dotted line marks the location of the lipids polar heads. The calculated helical content of (B) NKCS, (D) NKCS-[AA], and (F) NKCS-[LP] in the aqueous phase and near the membrane. Inner, outer, and water conformations are represented with different curves, as indicated. The helical content of the outer group of NKCS-[AA] is not shown since there were only 6 conformations (out of 3600). In all cases the helical content of the water conformations was the lowest and that of the inner conformations highest.

Additionally, the membrane-induced helix formation, as well as close electrostatic interactions between positively charged residues and the negatively charged membrane surface, made the "inner" group of conformations more favorable (Supporting Information Table S1).

On the basis of the preliminary simulations, we hypothesized that the membrane affinity depends on the compatibility of NKCS's sequence with an amphipathic helix structure and designed two peptides to examine this possibility (Table 1). In the first (NKCS-[AA]) we added two consecutive Ala residues into the hinge region of NKCS. With this, the polypeptide sequence becomes compatible with an amphipathic helix structure (Figure 2B) and the anticipation was that its membrane affinity would increase. Indeed, the simulations showed that the vast majority of the conformations, above 99% of total (Table 2), were embedded in the membrane with nonpolar residues within the hydrophobic core and the polar residues in the aqueous phase (Figure 1C). The helical content of these conformations was much higher than that of the original peptide and the only distortions were in the termini (Figure 1D). Reassuringly, the membrane affinity of NKCS-[AA] was much stronger than that of the original peptide (Table 2), as we hoped.

As a negative control experiment, we also designed a second variant (NKCS-[LP]) in which Leu-15 was replaced with a Pro. The idea was to interfere further with the helical structure of the peptide, thereby reducing its membrane affinity. Indeed, the

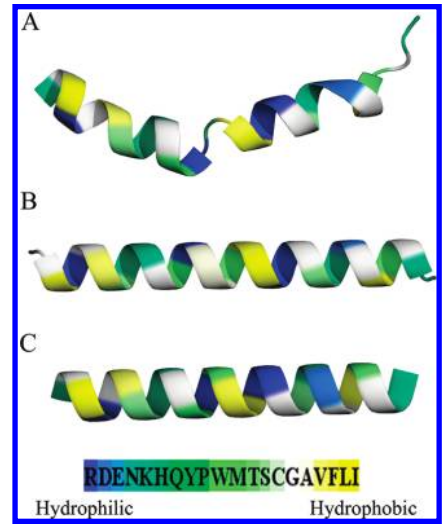

Figure 2. Compatibility of the peptide sequence with an amphipathic helical structure. The peptide is represented as ribbons colored according to the hydrophobicity scale in the bar. (A) Representative structure of NKCS in an "inner" conformation, obtained from the MC simulations in the membrane. The view is from the membrane surface upward, and the structure features two short amphipathic helices, connected by a hinge. (B) NKCS-[AA], constructed as a canonical α-helix. In contrast to NKCS, the sequence of NKCS-[AA] is consistent with the amphipathic helix structure. This is indeed the predominant conformation of the peptide in association with the membrane. The view is from the membrane plan upward, as in "A". (C) NKCS in a (hypothetical) canonical α-helix conformation. It is evident from the picture that the hydrophobic and polar/charged amino acids are spread in all directions and the conformation is not amphipathic. That is, NKCS's amino acid sequence is not compatible with an amphipathic helix structure.

NKCS-[LP] peptide associated with the membrane with less negative free energy than the original peptide NKCS (Table 2). Also here it was possible to distinguish between two groups of conformations. The outer group resembled that of NKCS in orientation and helical content. In both, the N-terminus up to Thr-13 was on average adsorbed on the surface of the membrane (Figure 1A,E) with quite high helical content (Figure 1B,F). The C-terminal region of NKCS-[LP], however, was located in the aqueous phase, and somewhat distorted, by design, due to the presence of Pro-15. Besides disruption of the α-helix, Pro-15 lowered the kink's flexibility, making the amphipathic arrangement of the peptide even less plausible than that of the original peptide.

To summarize, the conformations of the three peptides investigated in the simulations could be divided into two groups. The inner conformations were helical to various degrees, and amphipathic, with nonpolar residues facing the membrane. The outer conformations were much less helical and the interaction of the peptide with the membrane was maintained only by the Coulombic attraction between the positively charged Arg and Lys residues of the peptide with the membrane surface charge. According to the simulations, the membrane affinity of the peptide depended on the compatibility of its sequence with the amphipathic helix structure, in agreement with our hypothesis. Next we describe experiments that characterize the helicity of the three peptides and examine their membrane affinity and activity.

Experimental Results

CD Spectroscopy. To characterize the structure of NKCS, NKCS-[LP], and NKCS-[AA], we carried out CD experiments in the presence and absence of SDS. According to our results,

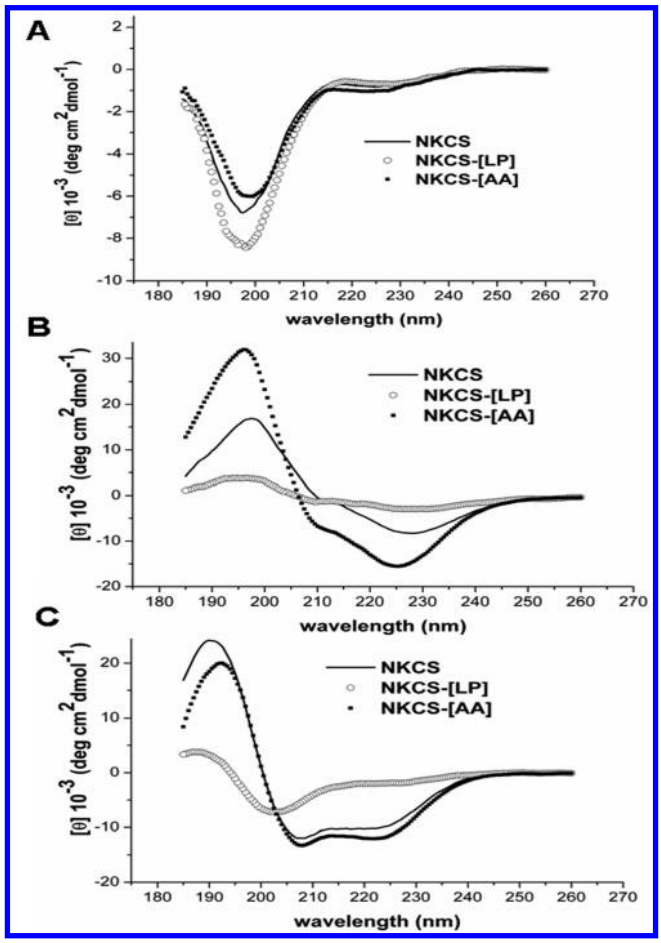

Figure 3. (A) CD measurements of NKCS and its derivatives in double distilled water. Negative bands in the region 198−200 nm and positive bands in the range 216−218 nm indicate disordered peptide structures. CD measurements of NKCS and its derivatives mixed with 1 mM (B) and 10 mM (C) SDS. The low concentration of detergent induced the adoption of ordered structures. At 10 mM SDS, NKCS and NKCS-[AA] clearly fold into α-helices (positive bands at 190−192 nm, negative bands at 208 and 222 nm). NKCS-[LP] is a mixture of β-sheet and random coils.

the three peptides were randomly coiled in water (Figure 3A). After the addition of the negatively charged SDS detergent, the adoption of a secondary structure was visible. Below the critical micelle concentration (CMC) of SDS, which is 8 mM, the peptides showed a preference toward the α-helical conformation (Figure 3B). The strong signal of NKCS-[AA] indicated a higher helical content in comparison with the two other peptides. At an SDS concentration above the CMC (10 mM), the helicity of NKCS and NKCS-[AA] increased (Figure 3C), but NKCS-[LP] seemed to adopt a mixture of random coils and β structures.

SPR. The interaction between the peptides and the lipid bilayer was investigated using the SPR method. The successful coating of the BIACore L1 chip by POPE was documented by the increase in the response units from 18200 to 24000 after rinsing with NaOH to wash away the unbound lipids (Figure 4A). The increase corresponded to a layer of thickness of 58 Å, similar to the thickness of a hydrated membrane obtained on the basis of SAXS measurements.

After injection of NKCS, a strong adsorption of the peptide was visible followed by a very slow desorption (Figure 4A). Such a behavior suggested a strong interaction between the peptide and POPE bilayers. The thickness of the peptide layer was estimated as 14 Å, corresponding to the diameter of an α-helix.[56,57] A different picture was observed after injection of

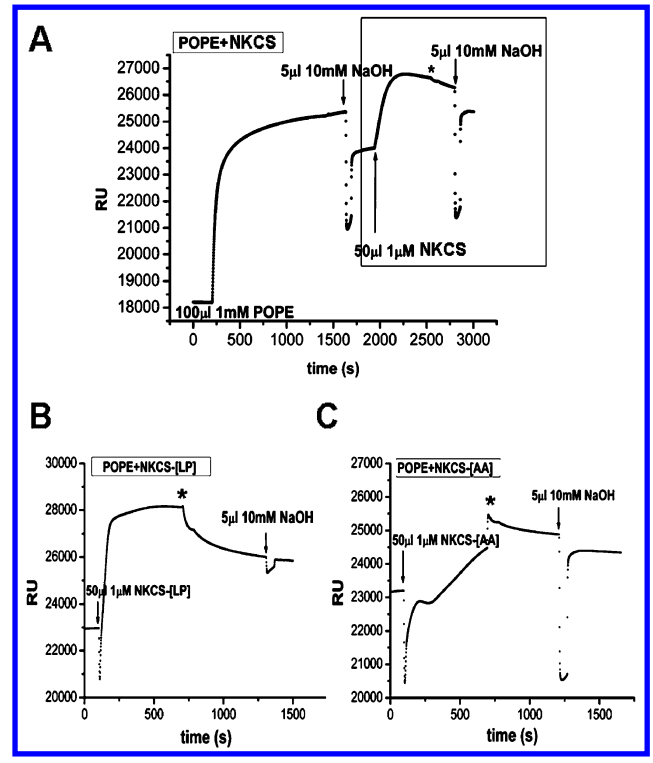

Figure 4. SPR measurements of the (A) NKCS, (B) NKCS-[LP], and (C) NKCS-[AA] peptides. Injections of POPE, NaOH, and peptides are indicated. The frame highlights the time range of the peptide−membrane interaction of NKCS with POPE. The onset was normalized to zero for NKCS-[LP] and NKCS-[AA]. The asterisks mark the end of the peptide injection and the beginning of peptide desorption. RU = response units.

NKCS-[LP] (Figure 4B). The peptide also adsorbed quickly. However, its desorption was very fast, which is indicative of a weaker affinity to the membrane than NKCS. The measurement allowed to estimate the peptide layer thickness as 29 Å.

The interaction of NKCS-[AA] with the POPE bilayer was more complicated (Figure 4C). After the injection of the peptide, its adsorption was very fast and strong but turned into a short desorption after 100 s. After an additional 80 s, a peptide adsorption occurred again. When the injection ended a slow desorption was observed. From the reference units (RU) one could approximate a peptide layer thickness of 12 Å, which corresponds to a single peptide layer. However, it should be stated that the determination of layer thickness from RU is a very difficult task and the reported values should be taken only as approximations.

For comparison, we determined the peptides' membrane affinity from the SPR sensograms, following previous studies.[22,58] The obtained values were similar to the computationally predicted ones, i.e., $-18.5kT$, $-16.1kT$, and $-25.7kT$ for NKCS, NKCS-[LP], and NKCS-[AA], respectively (Table 2).

SAXS Measurements. SAXS measurements were performed to investigate the influence of the peptides on the repeat distance (sum of lipid bilayer thickness and water layer between two lipid bilayers) and the inverse hexagonal phase transitions of POPE. All peptides changed the inverse hexagonal phase transition temperature of POPE liposomes (Supporting Information Figure S1 and Table 3) whereas the repeat distance, which was determined to be 55 ± 9 Å at 37 °C for POPE, remained the same within the error for all experiments (data not shown). All tested peptides shifted the transition temperature to higher values in a concentration dependent manner (Table 3). There

TABLE 3: Increase of the Inverse Hexagonal Phase Transition Temperature of a POPE Vesicles upon Interaction with NKCS Derivatives, Expressed as ΔT (°C)[a]

molar ratio [lipid/peptide]	NKCS	NKCS-[AA]	NKCS-[LP]
1000:1	4	3	4
300:1	10	5	5
100:1		9	6

[a] The aggregation of the sample POPE + NKCS in the molar ratio of 100:1 was so strong that the transfer into the measurement capillary was not possible.

TABLE 4: Antibacterial Activity of NKCS, NKCS-[AA], and NKCS-[LP] against *E. coli*, *S. carnosus*, and *B. subtilis* Determined as MIC (Minimal Inhibitory Concentration, μM)

peptide	*E. coli*	*S. carnosus*	*B. subtilis*
NKCS	0.63	2.5	1.25
NKCS-[AA]	1.25	2.5	2.5
NKCS-[LP]	2.5	5	5
melittin	2.5	0.63	0.63

was no effect on the pretransition between the gel and liquid crystalline phase for any of the peptides (data not shown).

Antibacterial and Hemolytic Activity. The three peptides NKCS, NKCS-[LP], and NKCS-[AA] and melittin (as a control) were tested against one Gram-negative and two Gram-positive bacteria strains and human erythrocytes. NKCS and its derivatives exhibited a good antibacterial activity against both types of bacteria, though they were slightly more active against the Gram-negative *E. coli* (Table 4). NKCS-[LP] showed an activity similar to that of melittin against *E. coli*, while NKCS and NKCS-[AA] were more potent. For the Gram-positive strains the minimal inhibitory concentration (MIC) of the three NKCS-based peptides was higher than the MIC of melittin. The peptides showed low hemolytic activity in comparison to melittin. At the very high concentration of 100 μM, the NKCS-[LP] and NKCS-[AA] derivatives caused lysis of 44.5% and 36.9% of red blood cells, respectively. The hemolytic activity of NKCS reached only 19.6% (Supporting Information Figure S2).

Discussion

In the present study we designed two cationic peptides based on NKCS, the 27-amino-acid fragment encompassing the membrane-active core region of NK-lysin. Their antibacterial and hemolytic activities, secondary structure, and interactions with model POPE membranes were investigated. The experiments were inspired by MC simulations.

Despite the overall good agreement between calculations and experiments in this study, it should be noted that our computational model has inherent limitations owing to its simplification of the complexity of the peptide−membrane interaction. First, the model treats the interaction of a single peptide molecule with the lipid bilayer and is not suitable (in its current form) for the study of peptide concentration effects, which are key to the understanding of antimicrobial peptide's membranolysis. Thus, the simulations are suitable only for results obtained at low peptide concentration. Second, the model membrane is planar (although free to change its width). Thus, membrane curvature effects, which are anticipated in the presence of POPE lipids, cannot be simulated. Third, both the peptide and membrane are described using a reduced representation, providing a procedure that is computationally feasible. However, it does not allow studies of specific peptide−lipid interactions in atomic details. Hydrogen bonds and salt bridges between the peptide and lipid, as well as the exact stereochemistry of the interaction, are not taken into account explicitly.

According to previous studies,[16] our CD measurements, and the MC simulations, NKCS was mostly unstructured in water but adopted an α-helical conformation in the membrane-mimetic environment. Moreover, the simulations of the peptide in POPE membranes showed a helix disruption at residues Thr-13 and Leu-14. The origin of this break in the helicity becomes clear when the peptide was presented as a canonical α-helix (Figure 2C). Two distinct hydrophobic faces, of the N- and C-termini, are oriented in different directions; i.e., the hydrophobic moments of the termini do not point in the same direction. Upon membrane interaction, this would not be a favorable conformation. However, the analysis of the computationally predicted inner conformations revealed that the kink in the middle allowed a deviation from a regular α-helix to a conformation with an improved amphipathic organization of the peptide. The kink enabled the helices in the N- and C-termini to align their hydrophobic moments so that the hydrophobic regions of both were oriented toward the membrane (Figure 2A).

The replacement of Leu-15 with Pro in NKCS-[LP] was assumed to perturb the α-helix even further, and both the CD measurements and the simulations supported this notion. NKCS-[LP] was found to be significantly less helical than NKCS, which can explain the reduced membrane affinity of this peptide in comparison to NKCS (Table 2). The weaker helicity of NKCS-[LP] can be correlated with the lower impact on the inverse hexagonal phase transition of POPE. Moreover, the SPR experiment showed a peptide layer of 29 Å, which is larger than the diameter of an α-helix.[56,57] This result can be correlated with the MC simulations that showed that while NKCS-[LP]'s N-terminus was embedded in the membrane, the C-terminus fluctuated above the surface (Figure 1E), resulting in an apparent thicker peptide layer.

The addition of two Ala residues into the sequence of NKCS was surmised to increase the α-helicity and improve the amphipathicity of the peptide, creating a single uninterrupted hydrophobic face (NKCS-[AA]; Figure 2B). The SPR experiments showed an association of NKCS-[AA] with the POPE membrane. The measured peptide layer thickness of 12 Å corresponds, approximately, to the average diameter of an α-helix, in agreement with the MC simulations. The computed and measured membrane-association free energy of NKCS-[AA] was much more negative (favorable) than that of NKCS (Table 2). Thus, we expected NKCS-[AA] to interfere more strongly with the membrane structure and to be more active against bacteria. However, the SAXS studies at various lipid−peptide ratios revealed consistently that the impact of NKCS-[AA] on the POPE bilayer structure was weaker than that of NKCS. The results also showed that NKCS-[AA] was slightly less active against bacteria than NKCS.

The three peptides shifted the temperature of inverse hexagonal phase transition to higher values. Observations of the peptide-induced lipids phase behavior can give an indication about membrane disruption. A temperature reduction suggests the generation of a negative membrane curvature whereas a high transition temperature indicates stiffening of the membrane and the induction of a positive curvature. The POPE lipid promotes spontaneous negative curvature,[59] and the adsorption of NKCS and its derivatives balanced this tendency and stabilized the bilayer. When the threshold concentration of the peptide was reached, a strong perturbation of the membrane occurred, leading eventually to lysis.[17,60]

This study was performed to examine the hypothesis that α-helicity and amphipathicity are the major structural features determining the membrane affinity of cationic antimicrobial peptides. We designed two peptides, based on the primary structure of NKCS. By exchanging (NKCS-[LP]) or inserting amino acids (NKCS-[AA]), we altered the α-helical content and amphipathicity of the peptide. Our CD and SPR measurements were in keeping with the Monte Carlo simulations regarding the secondary structure and membrane affinity of the peptides. Moreover, NKCS-[LP] showed a decreased antimicrobial activity and weak influence on POPE's hexagonal phase transition temperature, in comparison to NKCS, which correlated well with its lower (calculated and measured) membrane affinity. In contrast, the increase in the membrane affinity of the NKCS-[AA] peptide in comparison to that of NKCS did not result in increased membrane-lytic potency. Quite the contrary, the peptide was slightly less active than the original NKCS (Tables 3 and 4).

Antimicrobial and membranolytic activity correlate with membrane affinity; the affinity must be high enough for the peptide to associate with the membrane. Indeed, NKCS-[LP], which showed a reduced membrane affinity in comparison to NKCS also exhibited a reduced activity. However, NKCS-[AA] demonstrated approximately the same activity as NKCS in spite of its increased membrane affinity, implying that activity depends also on other factors. Perhaps the membrane adsorption of a kinked peptide, such as NKCS, can cause more significant membrane disruption than a perfect α-helix, such as NKCS-[AA]. In this respect, it is noteworthy that a cyclic analog of melittin (which retained the overall helical structure) showed reduced membrane affinity but increased activity.[61]

Conclusions

Overall, the present study demonstrates how the interplay between simulations and experiments can be combined to provide a molecular picture of the membrane interaction of NKCS. The next challenge is to understand the mechanism of membrane lysis. For that, it is necessary to replace the crude representation of the membrane that was used here by a molecular (perhaps even atomistic) model.

Acknowledgment. We gratefully acknowledge the assistance of Sadasivam Jeganathan (Max-Planck-Arbeitsgruppe "Zytoskelett" of Prof. Dr. E. Mandelkow in Hamburg) for CD measurements. We thank Prof. Dr. P. Dubruel from the Department of Organic Chemistry at Ghent University for supporting us with the SPR knowledge and equipment. This work was financially supported by the European Commission under the sixth Framework Program through the Marie-Curie Action: BIOCONTROL, contract number MCRTN-33439 and German-Israeli Foundation for Scientific Research and Development, grant number 831/2004.

Supporting Information Available: Detailed description of computational methods, a table of energy decomposition data, and two figures showing SAXS patterns and hemolytic activity diagram are provided. This material is available free of charge via the Internet at http://pubs.acs.org.

References and Notes

(1) Cohen, M. L. *Science* **1992**, *257*, 1050–5.
(2) Hamilton-Miller, J. M. *Int. J. Antimicrob. Agents* **2004**, *23*, 209–12.
(3) Powers, J. P.; Hancock, R. E. *Peptides* **2003**, *24*, 1681–91.
(4) Bush, K.; Macielag, M.; Weidner-Wells, M. *Curr. Opin. Microbiol.* **2004**, *7*, 466–76.
(5) Shai, Y. *Curr. Pharm. Des.* **2002**, *8*, 715–25.
(6) Zasloff, M. *Nature* **2002**, *415*, 389–95.
(7) Epand, R. M.; Shai, Y.; Segrest, J. P.; Anantharamaiah, G. M. *Biopolymers* **1995**, *37*, 319–38.
(8) Shai, Y. *Trends Biochem. Sci.* **1995**, *20*, 460–4.
(9) Shai, Y.; Oren, Z. *Peptides* **2001**, *22*, 1629–41.
(10) Matsuzaki, K. *Biochim. Biophys. Acta* **1999**, *1462*, 1–10.
(11) Andra, J.; Leippe, M. *Med. Microbiol. Immunol.* **1999**, *188*, 117–24.
(12) Jacobs, T.; Bruhn, H.; Gaworski, I.; Fleischer, B.; Leippe, M. *Antimicrob. Agents Chemother.* **2003**, *47*, 607–13.
(13) Olak, C.; Muenter, A.; Andra, J.; Brezesinski, G. *J. Pept. Sci.* **2008**, *14*, 510–7.
(14) Schroder-Borm, H.; Bakalova, R.; Andra, J. *FEBS Lett.* **2005**, *579*, 6128–34.
(15) Willumeit, R.; Kumpugdee, M.; Funari, S. S.; Lohner, K.; Navas, B. P.; Brandenburg, K.; Linser, S.; Andra, J. *Biochim. Biophys. Acta* **2005**, *1669*, 125–34.
(16) Andra, J.; Monreal, D.; Martinez de Tejada, G.; Olak, C.; Brezesinski, G.; Gomez, S. S.; Goldmann, T.; Bartels, R.; Brandenburg, K.; Moriyon, I. *J. Biol. Chem.* **2007**, *282*, 14719–28.
(17) Lohner, K.; Prenner, E. J. *Biochim. Biophys. Acta* **1999**, *1462*, 141–56.
(18) Haris, P. I.; Chapman, D. *Biopolymers* **1995**, *37*, 251–63.
(19) Ladokhin, A. S.; Selsted, M. E.; White, S. H. *Biophys. J.* **1997**, *72*, 794–805.
(20) Salditt, T.; Li, C.; Spaar, A. *Biochim. Biophys. Acta* **2006**, *1758*, 1483–98.
(21) Bechinger, B. *Biochim. Biophys. Acta* **1999**, *1462*, 157–83.
(22) Papo, N.; Shai, Y. *Biochemistry* **2003**, *42*, 458–66.
(23) La Rocca, P.; Biggin, P. C.; Tieleman, D. P.; Sansom, M. S. *Biochim. Biophys. Acta* **1999**, *1462*, 185–200.
(24) Forrest, L. R.; Sansom, M. S. *Curr. Opin. Struct. Biol.* **2000**, *10*, 174–81.
(25) Kessel, A.; Cafiso, D. S.; Ben-Tal, N. *Biophys. J.* **2000**, *78*, 571–83.
(26) Kessel, A.; Haliloglu, T.; Ben-Tal, N. *Biophys. J.* **2003**, *85*, 3687–95.
(27) Milik, M.; Skolnick, J. *Proteins* **1993**, *15*, 10–25.
(28) Baumgartner, A. *Biophys. J.* **1996**, *71*, 1248–55.
(29) Efremov, R. G.; Nolde, D. E.; Vergoten, G.; Arseniev, A. S. *Biophys. J.* **1999**, *76*, 2448–59.
(30) Ducarme, P.; Rahman, M.; Brasseur, R. *Proteins* **1998**, *30*, 357–71.
(31) Maddox, M. W.; Longo, M. L. *Biophys. J.* **2002**, *82*, 244–63.
(32) Veresov, V. G.; Davidovskii, A. I. *Eur Biophys J* **2007**, *37*, 19–33.
(33) Tzlil, S.; Murray, D.; Ben-Shaul, A. *Biophys. J.* **2008**, *95*, 1745–57.
(34) Wee, C. L.; Sansom, M. S.; Reich, S.; Akhmatskaya, E. *J. Phys. Chem. B* **2008**, *112*, 5710–7.
(35) Kessel, A.; Shental-Bechor, D.; Haliloglu, T.; Ben-Tal, N. *Biophys. J.* **2003**, *85*, 3431–44.
(36) Shental-Bechor, D.; Kirca, S.; Ben-Tal, N.; Haliloglu, T. *Biophys. J.* **2005**, *88*, 2391–402.
(37) Shental-Bechor, D.; Haliloglu, T.; Ben-Tal, N. *Biophys. J.* **2007**, *93*, 1858–71.
(38) Gordon-Grossman, M.; Gofman, Y.; Zimmermann, H.; Frydman, V.; Shai, Y.; Ben-Tal, N.; Goldfarb, D. *J. Phys. Chem. B* **2009**, *113*, 12687–95.
(39) Wang, X.; Quinn, P. J. *Biochim. Biophys. Acta* **2002**, *1564*, 66–72.
(40) Siegel, D. P. *Biophys. J.* **2006**, *91*, 608–18.
(41) van den Brink-van der Laan, E.; Killian, J. A.; de Kruijff, B *Biochim. Biophys. Acta* **2004**, *1666*, 275–88.
(42) Ames, G. F. *J. Bacteriol.* **1968**, *95*, 833–43.
(43) Bishop, D. G.; Rutberg, L.; Samuelsson, B. *Eur. J. Biochem.* **1967**, *2*, 448–53.
(44) Koch, H. U.; Haas, R.; Fischer, W. *Eur. J. Biochem.* **1984**, *138*, 357–63.
(45) Matsuzaki, K.; Sugishita, K.; Ishibe, N.; Ueha, M.; Nakata, S.; Miyajima, K.; Epand, R. M. *Biochemistry* **1998**, *37*, 11856–63.
(46) Hallock, K. J.; Lee, D. K.; Ramamoorthy, A. *Biophys. J.* **2003**, *84*, 3052–60.
(47) Szule, J. A.; Rand, R. P. *Biophys. J.* **2003**, *85*, 1702–12.
(48) Angelova, A.; Ionov, R.; Koch, M. H.; Rapp, G. *Arch. Biochem. Biophys.* **2000**, *378*, 93–106.
(49) Tytler, E. M.; Segrest, J. P.; Epand, R. M.; Nie, S. Q.; Epand, R. F.; Mishra, V. K.; Venkatachalapathi, Y. V.; Anantharamaiah, G. M. *J. Biol. Chem.* **1993**, *268*, 22112–8.

(50) Petrey, D.; Xiang, Z.; Tang, C. L.; Xie, L.; Gimpelev, M.; Mitros, T.; Soto, C. S.; Goldsmith-Fischman, S.; Kernytsky, A.; Schlessinger, A.; Koh, I. Y.; Alexov, E.; Honig, B. *Proteins* **2003**, *53*, 430–5.
(51) Blondelle, S. E.; Houghten, R. A. *Pept. Res.* **1991**, *4*, 12–8.
(52) Hall, K.; Mozsolits, H.; Aguilar, M. I. *Lett. Pept. Sci.* **2003**, *10*, 475–485.
(53) Cooper, M. A.; Hansson, A.; Lofas, S.; Williams, D. H. *Anal. Biochem.* **2000**, *277*, 196–205.
(54) *Real-Time Analysis of biomolecular interactions: applications of BIACORE*; Nagata, K., Handa, H., Eds.; Springer Publishing Co.: New York, 2000.
(55) Boulin, C.; Kempf, R.; Koch, M. H. J.; McLaughlin, S. M. *Nucl. Instrum. Methods.* **1986**, *249*, 399–407.
(56) Vie, V.; Van Mau, N.; Chaloin, L.; Lesniewska, E.; Le Grimellec, C.; Heitz, F. *Biophys. J.* **2000**, *78*, 846–56.
(57) Ambroggio, E. E.; Separovic, F.; Bowie, J.; Fidelio, G. D. *Biochim. Biophys. Acta* **2004**, *1664*, 31–7.
(58) Mozsolits, H.; Thomas, W. G.; Aguilar, M. I. *J. Pept. Sci.* **2003**, *9*, 77–89.
(59) Fuller, N.; Rand, R. P. *Biophys. J.* **2001**, *81*, 243–54.
(60) Bechinger, B.; Lohner, K. *Biochim. Biophys. Acta* **2006**, *1758*, 1529–39.
(61) Unger, T.; Oren, Z.; Shai, Y. *Biochemistry* **2001**, *40*, 6388–97.

JP909154Y